Item 18 of 37

Our Number 8049052

Their Number 8043783

Printed Date 04 Aug 2010

Request From Geoscience Australia

Service 1		Service 2	
Service Type	Copy non returnable	Service Type	Copy non returnable
Media Type	Photocopy	Media Type	None

Bibliographic Details

Author Acoustical Society of America
Title The Journal of the Acoustical Society of America.
ISBN/ISSN 0001-4966 1
Control Number BRN 75208, J10580000, sn 78000654
Publisher American Institute of Physics for the Acoustical Society of America.
Call Number <BRN 75208>
Verification source Libraries Australia/.biball-r20-db04

HK Serial

Article Details

Volume/Issue 91/6
Article Title Development of the active doublet method for measuring
Article Author Roberts, et.al
Article Date 1992
Pagination 3291-3302

QC 221. A24

Service Level Core
Item Format Print Journal
Request Created Date 03 Aug 2010 14:01
Expiry Date 10 Aug 2010
Name
Email
Delivery Method Electronic Mail

Supplied: ....
Photocopy Printout
Number of Pages: ....
Mail Fax Ariel

Date Note

Rota NLA: AMG

Send To
Delivery Address

ill.library@ga.gov.au
Geoscience Australia Inter Library Loans
Cnr Jerrabomberra Ave and Hindmarsh

Development of the active doublet method for measuring small velocity and attenuation changes in solids

Peter M. Roberts, W. Scott Phillips, and Michael C. Fehler
Earth and Environmental Sciences Division, Geoengineering Group, EES-4, Mail Stop D443, Los Alamos National Laboratory, Los Alamos, New Mexico 87545

(Received 25 November 1991; accepted for publication 24 February 1992)

The measurement of small changes in elastic wave velocity and attenuation is important to a broad range of problems, such as earthquake prediction and early detection of rock failure in mines. Previous authors proposed a method for estimating small temporal velocity changes in the earth's crust by analyzing progressive relative phase delays between the scattered waves of two signals generated by nearly identical earthquake sources, called doublets, recorded at different times at the same receivers. Several improvements have been made to the original method and are presented here. The reliability of measured velocity changes has been increased by using active, repeatable sources instead of natural earthquakes. The robustness of the analysis technique has been improved by eliminating unnecessary intermediate phase regression steps and thus reducing the sensitivity to spurious data. Finally, the phase-delay algorithm has been extended to allow measurement of small attenuation changes from relative amplitude decay rates. Using ultrasonic source and receiver transducers embedded in Plexiglas test samples, velocity changes as small as 0.01%, caused by ambient temperature variations in the Plexiglas, have been measured. Changes in attenuation on the order of 10%, due to permanent damage induced in one of the samples, have also been measured.

PACS numbers: 43.35.Pt, 43.20.Jr, 43.40.Ph

INTRODUCTION

Temporal changes in elastic wave velocity and attenuation can provide important precursory information about stress accumulation preceding major earthquakes. For instance, Sato[1] observed a change in crustal attenuation preceding the Western Nagano earthquake in Japan. Measurements of temporal changes are also important for detecting and characterizing the migration of fluids and gas in hydrocarbon and geothermal reservoirs[2] because this knowledge can help improve production efficiency and allow estimation of reservoir lifetime. Localized velocity and attenuation changes in mine walls can provide early indications of possible failure conditions. The usefulness of temporal changes, however, is limited by the accuracy and precision with which velocity and attenuation measurements can be made. The higher the measurement precision is, the lower the threshold becomes for detecting velocity and attenuation changes. Lower detection thresholds allow characterization of earlier or more subtle physical changes taking place within the study region.

Poupinet *et al.*[3] presented a high-precision method for measuring temporal velocity changes in the earth's crust. The method compares the scattered wave portions, or coda,[4] of two highly similar waveforms, recorded at the same receiver at different times, which were generated by a pair of nearly identical sources, called doublets. Although the term "doublet" strictly refers to a single pair of identical sources, we will use it to describe any repeatable source, regardless of how many events occurred. We will also refer to the basic technique of comparing the highly similar scattered waves generated by such sources as "the doublet method." By analyzing progressive relative phase delays between the two doublet signals as a function of elapsed time, defined relative to the source origin times, Poupinet *et al.*[3] proposed that, with sufficiently accurate recording equipment, measurements of velocity changes on the order of 0.01% could be made. Such small velocity changes usually cannot be detected from travel-time delays obtained for individual arrivals unless repeatable sources are used that allow either signal stacking or averaging of many relative time delay measurements.[5,6] Although source repeatability is required for the doublet method to be successful, it does not, in general, require averaging to achieve the high measurement precision. Only two signals are compared at a time, but these signals must be nearly identical and this is the only reason why the source must be repeatable. The high precision of the doublet method is possible because coda waves sample regions of interest redundantly and generally follow paths that increase in length with elapsed time.[4]

In this paper, we assume the scattered waves are composed of only a single wave type, e.g., compressional or shear, so that complicated effects of mixed waves traveling with different velocities can be ignored. We also assume that changes in velocity dispersion are negligible. Although plates are well known to support dispersive waves over the range of frequencies that we examined,[7] our data indicated that the velocity changes we measured were independent of frequency, implying that the velocity dispersion curve shifted up or down with little change in its overall shape. Thus a small decrease in velocity occurring within the sampled region during the time period between the doublet origin times

 0001-4966/92/063291-12$00.80

will produce a relative delay that increases with elapsed time over some portion of the scattered waves. If the velocity change is pervasive the relative delay will increase linearly over the entire coda. This trend of increasing delay is easier to detect and measure than an isolated delay based on a single arrival.

Prior to the work of Poupinet *et al.*[3] signals from natural earthquake doublets had been identified and studied by other investigators,[8,9] but no method was proposed for analyzing the details of the scattered waves. Little work has been done with earthquake doublets for three main reasons. First, naturally occurring doublets in the earth are difficult to find. Second, even when natural doublets are found, there is no guarantee that the source location was absolutely identical for both events, and this leads to ambiguous interpretations of any measured phase delays. Finally, the algorithm used by Poupinet *et al.*[3] is not robust enough to give reliable measurements without first inspecting the numerous intermediate results of the analysis. Other investigators have used the phase-delay technique on individual arrivals from similar waveforms to obtain high-precision relative locations for earthquakes,[10,11] but the scattered waves were not analyzed. However, Karageorgi *et al.*[12] used a time-domain cross-correlation version of the doublet method to investigate changes in anisotropy and near-source seasonal water table variations at Parkfield using active Vibroseis® sources. In that study, significant relative delays were observed in the later portions of the coda wave trains for signals acquired repeatedly over a period of several years.

With the purpose of developing a new diagnostic tool for studying subtle changes in earth properties as motivation, we conducted controlled laboratory ultrasonics experiments in Plexiglas samples. These experiments were guided by the goals of eliminating the source location ambiguities that have hindered previous natural doublet studies, developing and improving the analysis method itself, and applying the improved method to the scattered wave portions of doublet signals to measure small velocity and attenuation changes induced in the sampled medium. We have achieved all three of these goals by (1) using active repeatable pulsed sources for generating signals in the test samples, (2) implementing several changes in the doublet analysis algorithm that increase its stability and decrease user interaction, and (3) inducing controlled physical changes in the Plexiglas samples and measuring the corresponding velocity and attenuation changes using the improved algorithm.

Preliminary results of this work were presented by Roberts.[13] In this paper, we describe our laboratory experiments and give a brief review of the original Poupinet *et al.*[3] method. Next, we discuss the improvements we have made to the phase-delay algorithm and show examples of small velocity changes we measured in Plexiglas test samples. We then describe the amplitude-decay algorithm and show examples of measured Q^{-1} changes. Finally, we give a brief discussion of possible applications of the active doublet method to scaled-up *in situ* crustal studies in the earth.

I. DESCRIPTION OF LABORATORY EXPERIMENTS

In our laboratory tests, we used identical source–receiver combinations to collect ultrasonic signals before and after altering the physical properties of Plexiglas test samples. We will show results for two Plexiglas samples; a 24-in.-square by 1/2-in.-thick plate, and a smaller plate approximately 10 in. square by 1/4 in. thick. Source repeatability was achieved by placing transducers in counter-bored holes in the samples and then filling the holes with epoxy. The transducers used were Valpey-Fisher 1.0-MHz PZT-4 disks with diameters from 1/8 in. up to 1/2 in. A variety of transducer locations were tested initially to investigate the dependence of the scattered wave field on source–receiver position. For our purposes, the specific choice for source and receiver was irrelevant because the scattered waves sampled virtually the entire plate in all cases.

Figure 1 shows a schematic of the test apparatus that we assembled to generate and record doublet signals in the two samples. We used half-cycle cosine pulses as source function inputs. Source pulse widths used were 6.67 μs for the thicker plate and 5.0 μs for the thin plate. Scattered waves are generated by multiple reflections at the four edges of the Plexiglas plates. Figure 2 shows a typical test signal acquired with the

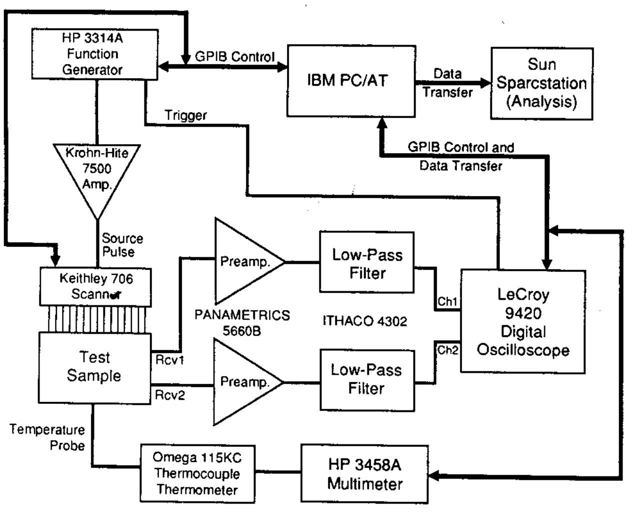

FIG. 1. Schematic block diagram of experimental apparatus used to generate and record doublet signals in laboratory test samples, and to monitor ambient sample temperature.

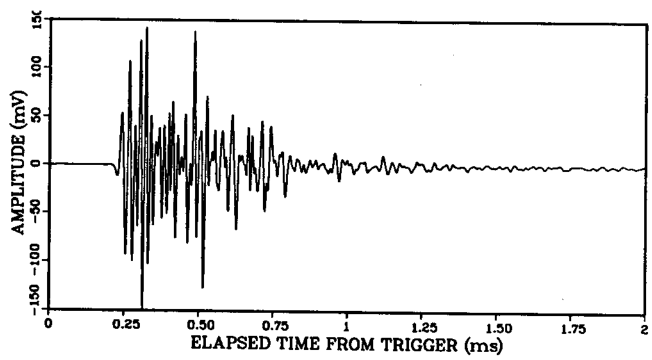

FIG. 2. A typical ultrasonic test signal generated by pulsing one piezoelectric transducer and receiving on another. The source and receiver were located on opposite ends of the thick Plexiglas sample with a separation of 50.8 cm. The direct arrival is followed immediately by scattered (coda) waves, which are exploited in the doublet analysis.

source and receiver located at opposite ends of the thick Plexiglas sample. The direct-path distance was 50.8 cm and the travel time of the first motion for the direct arrival was measured to be 0.18 ms. This gives a compressional wave velocity of approximately 2820 m/s for Plexiglas. The doublet method analyzes the long tail of scattered waves, or coda, following the direct arrival. Velocity and attenuation changes that we measured in our test samples were caused by ambient temperature variations in the thicker sample, which is a reversible process, and by permanently damaging large portions of the thin sample by exposure to extreme heat. We used data from these experiments to test and improve the phase-delay techniques and the amplitude-decay method.

II. THE ORIGINAL PHASE-DELAY METHOD

The basic method of doublet analysis as originally described by Poupinet *et al.*[3] involves incrementing a data window through both doublet signals simultaneously. A Fourier transform is then computed using the fast Fourier transform (FFT) algorithm for each windowed signal at each time step. For each pair of data windows, the cross spectrum is obtained by multiplying the Fourier transform of one signal by the complex conjugate of the other:

$$S_{12}(t,f) = S_1(t,f)S_2^*(t,f), \tag{1}$$

where $S_1(t,f)$ and $S_2(t,f)$ are the Fourier transforms of the two windowed signals at elapsed time t, $S_{12}(t,f)$ is their cross spectrum, and the asterisk indicates complex conjugation. The phase of S_{12} for progressively later time windows is used to obtain the relative signal delay as a function of elapsed time, beginning at the first arrival and extending through the coda. This, in turn, leads to estimates of relative changes in velocity $\Delta V/V$ if the signal delay versus elapsed time follows a linear relation over some portion of the coda. If the linear trend persists over the entire coda, then the velocity change is pervasive throughout the sampled volume.

In Fig. 3(a)–(c), we show an example illustrating the basic moving-window technique and the original algorithm used by Poupinet *et al.*[3] for obtaining $\Delta V/V$ from progressive phase delays. At the top of Fig. 3(a), we show two ultrasonic signals generated by the 6.67-μs pulsed source in the thicker Plexiglas plate and recorded with a sampling interval

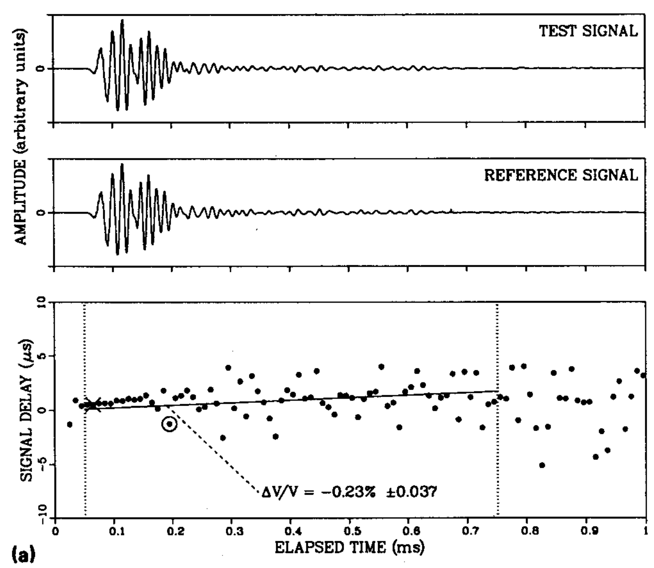

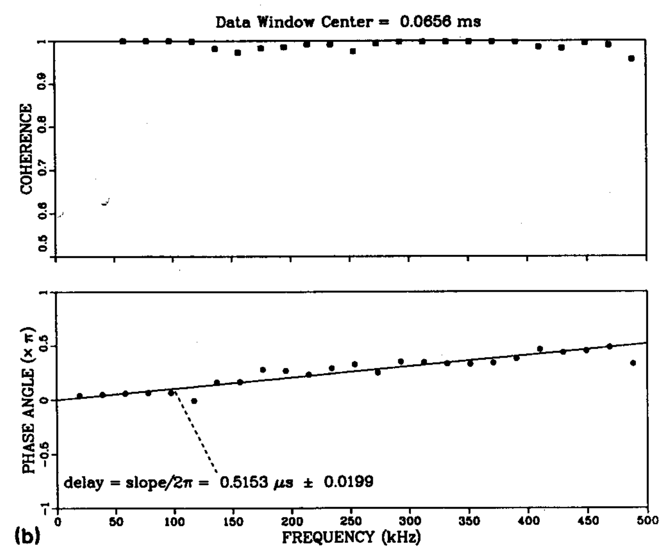

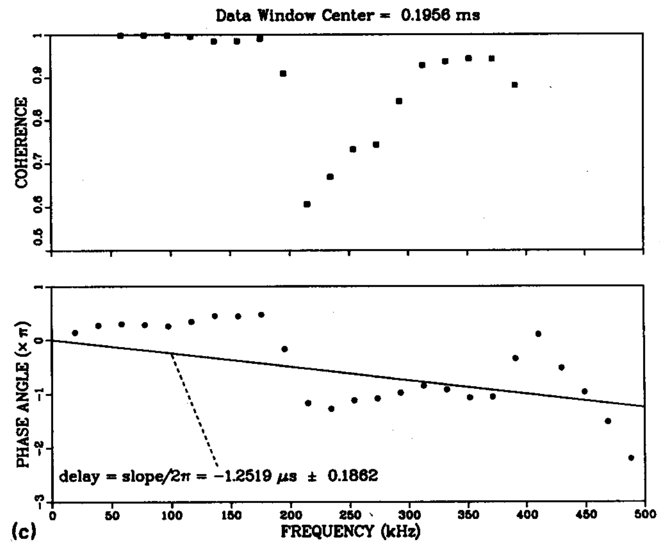

FIG. 3. (a) Results of the unmodified Poupinet *et al.*[3] doublet algorithm applied to a doublet pair (top) generated in a Plexiglas plate in our laboratory. The two signals were acquired before and after a change in ambient temperature occurred in the laboratory. The delays versus elapsed time (bottom) were measured for the test signal relative to the reference signal. Each delay point was obtained by a separate linear regression on cross-spectral phase for the corresponding time window, as shown in the next two figures. The delay versus time regression, used to estimate $\Delta V/V$, was applied only within the 3:1 signal-to-noise limits indicated by the vertical dashed lines. (b) Example of linear regression performed on cross-spectral phase versus frequency (bottom) for an early time window near the first arrivals. The slope of the regression line yielded the signal delay point marked with a large "×" in (a). The coherence spectrum (top) was used to weight phase data points in the regression. The delay value is small enough in magnitude that the phase has not exceeded the $+\pi$ threshold before the cutoff frequency is reached. Thus it was not necessary to unwrap the phase curve in this case. (c) Same as (b) except phase versus frequency data are shown for a later time window in the coda, indicated by the circled point in (a). In this case, the discontinuity-detection algorithm for unwrapping phase (see text) was fooled by the spurious phase point just below 200 kHz. As a result the phase curve was unwrapped in the wrong direction and this produced an erroneous negative time delay.

of 50 ns. The same source and receiver transducers were used, but the two signals were acquired on different days. For this test, the source and receiver were both located at one edge of the plate with a separation of 15.25 cm, yielding a direct-path travel time of 0.054 ms. The velocity changes that we observed were due to changes in ambient temperature in the laboratory, which was continuously measured and correlated with the results. For the moving window, we used a data width of 51.2 μs (1024 data points) and an increment of 10 μs between successive windows. Each data window was tapered with a Hanning cosine function. Plotted below the test signals are the relative delays calculated for each window pair. Each delay point was obtained by fitting a least-squares regression line to the cross-spectral phase versus frequency for each time window. This is illustrated in Fig. 3(b) for one time window, indicated by the delay point marked with a large "×" in Fig. 3(a). The principal assumption is that the two signals are identical in each time window t except that one may be delayed relative to the other. Thus their cross-spectral phase ϕ must be a linear function of frequency f, with a value of zero at the intercept. Then, the relative signal delay τ is directly proportional to the slope of the least-squares regression line fit to the relation

$$\phi(t,f) = 2\pi f \tau(t). \tag{2}$$

All phase points in each time window are reduced to a single delay point and plotted as in Fig. 3(a).

The coherence spectrum at the top of Fig. 3(b) is used to weight the phase points in the linear regression. Coherence is a measure of the similarity between the two doublet signals at each frequency and has a value of 1 when the signals are identical. We calculated coherence magnitude spectra using smoothed versions of the cross spectrum and autospectra in each time window and the following formula:[14]

$$\|C_{12}(t,f)\| = \frac{\|\hat{S}_{12}(t,f)\|}{[\hat{S}_{11}(t,f)\hat{S}_{22}(t,f)]^{1/2}}, \tag{3}$$

where S_{11} and S_{22} are the autospectra of the two signals and the caret indicates frequency-domain convolution with a five-point triangular smoothing window.

Note that the linear regression must be performed on continuous phase curves that either do not contain or have been corrected for the modulo(2π) ambiguities caused by computing the principal value of the arctangent function, which is defined over the range of $\pm\pi$. No mention of this potential problem was made by Poupinet *et al.*,[3] presumably because the delays they measured were not strong enough to cause the phase values to cross the $\pm\pi$ threshold for the frequency bands they examined. This is also the case in Fig. 3(b), but we will show below that phase wrapping can become a problem later in the coda and this will lead to one of our improvements to the algorithm in the next section.

In Fig. 3(a) the delay versus elapsed time is progressive with a linear trend out to approximately 0.15 ms. Since the source and receiver locations are fixed, this trend implies that a path-related change, either velocity or length, has occurred in the test sample. If the cause of the progressive delay is dominated by a velocity change $\Delta V/V$ and as long as $\tau \ll t$, then a second least-squares regression on the τ vs t data gives $\Delta V/V = -\Delta\tau/\Delta t$. We will refer to the original algorithm of Poupinet *et al.*[3] as the "two-step regression technique." For the doublet signals in Fig. 3(a), we applied this technique without first inspecting each intermediate phase regression step to try to identify and eliminate spurious delays caused by erratic phase data. We did, however, use signal-to-noise ratio estimates, averaged over the dominant frequency band of the signals, to restrict the range of delay points used in the $\Delta V/V$ regression. By fitting delays only within the range where the signal-to-noise ratio was higher than 3.0, indicated by the region inside the two vertical dashed lines, we estimated a velocity change of $\Delta V/V = -0.23\%$. This result is erroneous, though, because of large errors in the delay estimates for $t > 0.15$ ms.

The scatter in the later delays in Fig. 3(a) was caused by inadequate removal of the modulo(2π) phase ambiguities and could have been controlled by inspecting each ϕ vs f plot to ensure that the phase curves were correctly unwrapped. Because the slope of the ϕ vs f regression line is proportional to the signal delay, the frequency at which the phase first crosses the $\pm\pi$ threshold is inversely proportional to the delay magnitude. The first phase curve discontinuity caused by wrapping will occur at the first phase point for which $|f\tau| > 0.5$, because this gives $|\phi| > \pi$. If the only discontinuities in the phase curves are caused by wrapping then these can be removed by detecting the frequencies where sudden phase excursions occur and then adding or subtracting integer multiples of 2π to all phase points at higher frequencies. However, simple threshold-detection algorithms can be easily fooled by discontinuities caused by spurious phase points. This is illustrated in Fig. 3(c) which shows the phase regression results that yielded the delay point marked with a large open circle in Fig. 3(a). We set a threshold of $\pm 0.9\pi$ for detecting phase excursions considered to be caused by principle value discontinuities. The spurious phase point just below 200 kHz caused the unwrapping algorithm to detect a positive discontinuity at the next highest frequency, and thus 2π was subtracted from all phase data above the spurious point. This yielded an erroneous negative delay for this time window. Although more elaborate automatic techniques exist for unwrapping phase,[15] the requirement that the unwrapped phase curve must be a continuous function of frequency often causes problems when outlying phase points are present. Instead of trying to unwrap the phase, we could have set a cutoff frequency at approximately 175 kHz to improve the delay estimate in Fig. 3(c), but this would eliminate the useful high-coherence data between 300 and 400 kHz. Also, choosing the cutoff frequency requires inspection of each phase curve and we wish to reduce user interaction. Thus we need an automated method to use preset fixed limits for the cutoff frequency, signal-to-noise ratio and coherence for obtaining stable and accurate delay estimates. This necessarily requires a reliable algorithm for unwrapping phase and a means for avoiding the inspection and arbitrary truncation of cross-spectral phase curves.

III. IMPROVEMENTS TO THE ORIGINAL METHOD

The two-step technique fails to take full advantage of the principal assumption that, as long as dispersion and mixed wave type effects are negligible, the cross-spectral phase is linear with a value of zero at the intercept. This assumption allows us to eliminate the intermediate phase regression steps so that, instead of estimating a single delay point for each time window, we convert all phase data to units of equivalent time delay as

$$\tau(t,f) = \phi(t,f)/2\pi f. \qquad (4)$$

All phase-derived time delays are then plotted directly versus elapsed time. In this way, all usable phase data may be fit simultaneously to obtain $\Delta V/V$ in one step rather than two. This allows trends in the measured delays to be derived from the cross-spectral phase directly rather than from intermediate measurements based on the slope of the ϕ vs f curves. This is particularly useful for reducing errors caused by erratic phase data at lower frequencies when dealing with narrow-band data. This approach, which we will call the "one-step regression technique," also minimizes the influence that spurious outlying phase data have on the delay estimates and eliminates the need for manual inspection of intermediate ϕ vs f plots.

If the signal delay is progressive and linear, even if only over short portions of the scattered waves, we can use an initial estimate of its trend versus elapsed time as a guide for iteratively unwrapping the 2π ambiguities in the phase. Since we can add or subtract any integer multiple of 2π to each phase point, the ambiguity in the equivalent phase-derived time delays can be expressed as

$$\tau(t,f) = \phi(t,f)/2\pi f \pm n/f, \qquad (5)$$

where n is any non-negative integer. Thus individual time delays can be adjusted by integer multiples of $1/f$ until they lie as close as possible to the initial estimate. Because no continuity requirement is imposed on the ϕ vs f data, spurious phase points will not affect the resulting unwrapped time delays. The initial estimate of the delay trend could be based, for instance, on zero-crossing delays, on median values of the phase-derived time delays before unwrapping, or on time-domain cross correlation, none of which would give as stable a result as fitting the unwrapped converted phase data directly.

In Fig. 4(a), we show the initial results of applying the one-step technique to the same pair shown in Fig. 3(a), before attempting to unwrap the phase. The doublet signals at the top of Fig. 4(a) are now plotted on top of each other in different colors to better illustrate the progressive delay. At the bottom of Fig. 4(a) phase-derived time delays are plotted versus elapsed time and color coded according to frequency. Each colored square represents a single point on the ϕ vs f curve for the corresponding time window. Although the signals had peak frequencies at approximately 60 kHz, we set a high cutoff frequency at 500 kHz to demonstrate that reliable data can be selected over a wide bandwidth by eliminating all phase points having coherence or signal-to-noise ratio below preset thresholds of acceptability. Thus, although the frequency spacing for each cross spectrum was $\Delta f = 19.5$ kHz, in most of the time windows the number of spectral points plotted is less than the total computed out to 500 kHz. Typically the values we used for coherence and signal-to-noise thresholds were 0.9 and 3.0, respectively. However, to better illustrate the capability of the unwrapping technique, we set lower thresholds of 0.8 for coherence and 1.0 for signal-to-noise so that more phase data are shown in Fig. 4(a) than we would normally use.

The effects of phase wrapping are clearly seen in Fig. 4(a). The first obvious occurrence is at elapsed times of 0.1–0.2 ms, where for higher frequencies the phase-derived time delays have negative values because the corresponding phase values are in the range $0 > \phi \geqslant -\pi$. Thus the apparent frequency dependence of the delays in Fig. 4(a) is an artifact of the arctangent function and must be corrected for as described above. As two possible guidelines for unwrapping the phase, we determined the median value of the phase-derived time delays in each time window and also measured the relative time delay between the zero crossings of the two signals directly from the time series. We found it useful, in general, to examine more than one type of initial delay estimate because the success of each can depend on the data being analyzed. Reliable zero crossings are difficult to determine when the data are either noisy or the waveforms are complicated. Median delays can be erratic when the normal distribution of the converted phase values for a given time window has long tails corresponding to large numbers of outliers. The signals in the present example allowed reliable zero-crossing delays to be measured and we used these to obtain the initial estimate of $\Delta V/V$, as shown in Fig. 4(a). We then add or subtract multiples of $1/f$ to the phase-derived time delays until the adjusted values lie as close as possible to the initial estimate.

Figure 4(b) shows the results after one iteration of phase unwrapping, which is usually enough. Note that the negative delays seen before at 0.1–0.2 ms in Fig. 4(a) have been adjusted upward and now agree with the zero-crossing delay estimates. The final regression line on the adjusted phase data yielded a velocity change of $\Delta V/V = -0.80\%$, which is larger in magnitude than the estimate obtained by the two-step technique [cf. Fig. 3(a)]. This is the correct value because it agrees well with that obtained from the zero crossings. The two-step technique underestimated the velocity change because of erratic time delays based on incorrectly unwrapped phase curves. Note that, in general, time delays could be frequency dependent if strong changes in dispersion occur in the medium under test. This could happen if defects with sizes on the order of the wavelengths being used to test the material are introduced. If dispersive effects become significant, though, they will show up clearly in the time delay plots as a systematic increase or decrease of the delays with frequency in each time window. In these cases, the $\Delta V/V$ regression can be performed over multiple frequency bands, rather than fitting all frequencies simultaneously, so that dispersive changes in group velocity can be measured. Although there is significant scatter in the time delays in Fig. 4(b), the variations with frequency are not systematic enough to suggest that changes in dispersion are responsible. Because the scatter increases with elapsed time and has primarily a random distribution with frequency, we believe the variations are due to noise.

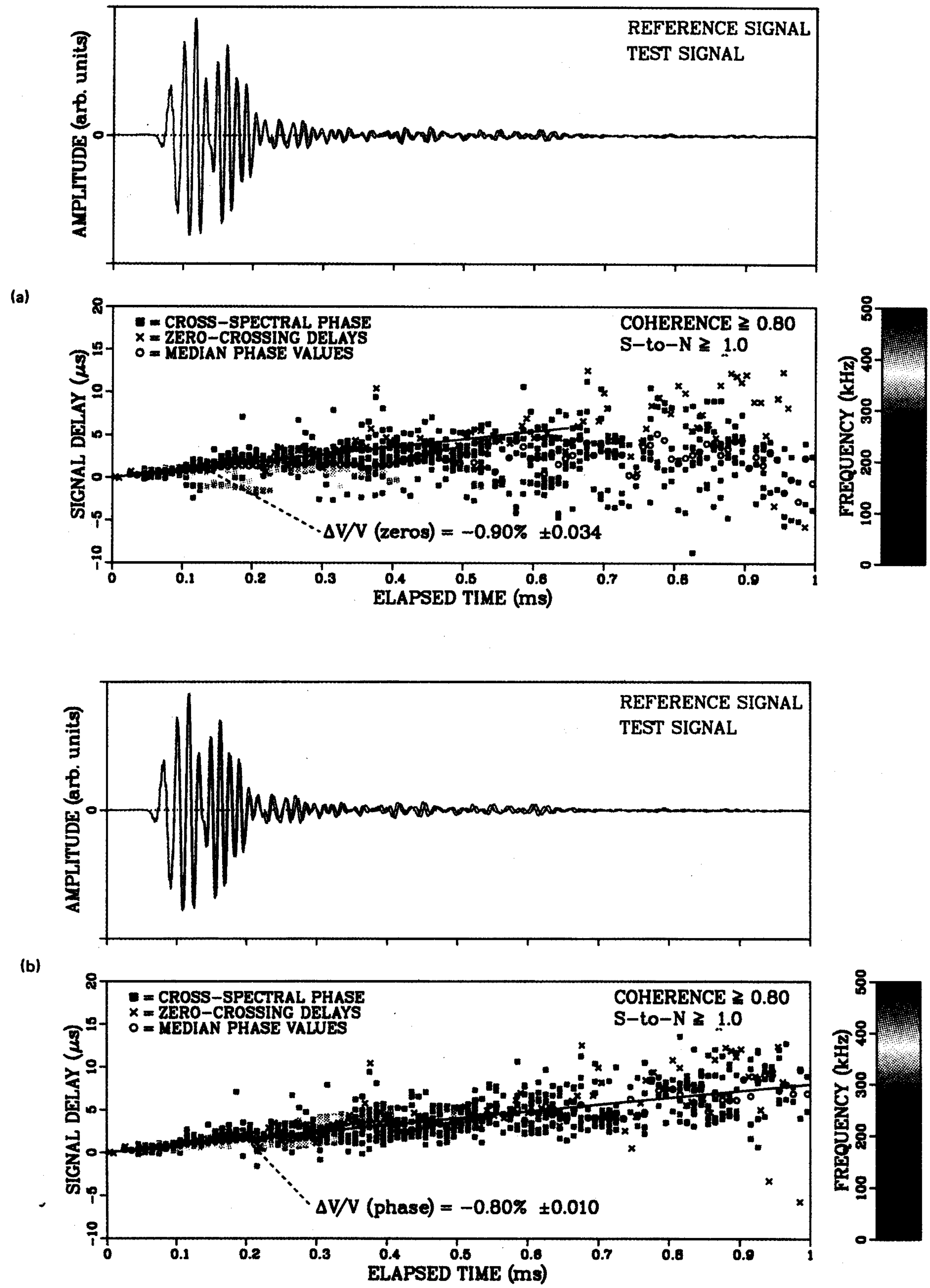

FIG. 4. (a) Results of the improved one-step doublet algorithm, before adjusting phase for modulo(2π) ambiguities, applied to the same doublet pair shown before in Fig. 3(a). All phase-derived time delays with coherence and signal-to-noise ratios above the indicated thresholds are plotted directly versus elapsed time and color coded by frequency. Median delay values and zero-crossing delays are superimposed on the phase-derived delays. The zero-crossing delays were used to obtain an initial estimate of $\Delta V/V$, shown at the bottom of the plot, to guide the phase unwrapping. The regression line that yielded this estimate is plotted over the range of zero-crossing delays that were used in the least-squares fit. (b) Same results as in (a) after one iteration of the phase adjustment algorithm. The final value for $\Delta V/V$ was obtained by fitting a least-squares line to the unwrapped, converted phase data with the zero-time intercept fixed at zero delay.

IV. VELOCITY CHANGES MEASURED IN PLEXIGLAS

The one-step technique has proved to be more robust than the original two-step method and is now quite easy to apply. Figure 5 summarizes velocity changes in the thick sample versus ambient temperature, which we measured with a thermocouple attached to the sample. In this case, measured "velocity changes" are a combination of true velocity variations due to changes in moduli and density, and dimensional changes due to thermal expansion or contraction. The sensitivity of the method and the reliability of the one-step algorithm are displayed clearly in Fig. 5. The smallest nonzero velocity change shown in this plot has a value of 0.01% with a standard error of $\pm 0.001\%$. The slope of $-0.165\%/{}^\circ\mathrm{C}$ that we obtained for velocity variations versus temperature is within range of possible values for Plexiglas: approximately $-0.01\%/{}^\circ\mathrm{C}$ for thermal expansion[16] and $-0.15\%/{}^\circ\mathrm{C}$ for the effects due to modulus and density changes.[17] The $\Delta V/V$ versus temperature results in Fig. 5 were obtained by applying the improved algorithm blindly to the numerous doublet pairs, without assuming any initial knowledge about the nature of the experiment or the frequency content of the data. Once we had chosen suitable analysis parameters such as window width and increment, all doublet signals were processed identically. A fixed cutoff frequency of 500 kHz was used throughout and potentially bad data were eliminated by using thresholds of 0.9 on coherence and 3.0 on signal-to-noise ratio.

We have also observed larger velocity variations due to permanent damage created by heating a portion of the Plexiglas in two progressive stages. We used the thin Plexiglas plate for this experiment with the 5.0-μs input source pulse width. The source and receiver were located at opposite edges of the plate with a separation of 22.0 cm, giving a direct-path travel time of 0.078 ms. The sampling interval used was 80 ns, the data window width was 81.92 μs and the increment between windows was 10 μs. The doublet signals

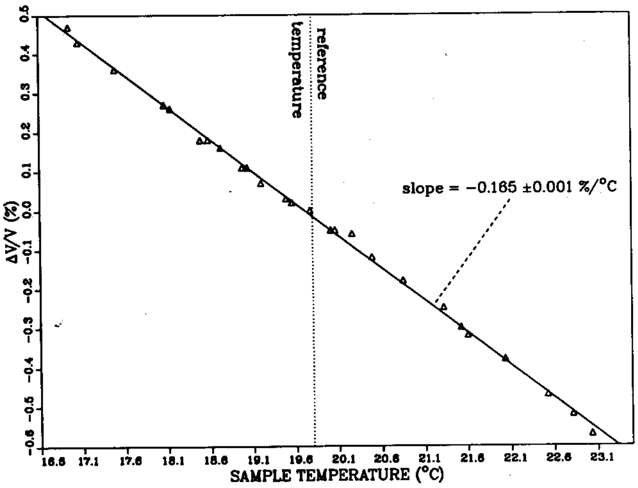

FIG. 5. Measured velocity changes in Plexiglas versus ambient sample temperature for numerous doublet pairs collected in the laboratory. This demonstrates the sensitivity and stability obtainable with the improved doublet algorithm, as well as the reliability of velocity changes measurable with the method.

used contained almost no coherent frequencies above 300 kHz, so we used this as the cutoff frequency and set the coherence and signal-to-noise thresholds at 0.9 and 3.0, respectively. The results are shown in Fig. 6(a) for the initial stage of damage where the sample was heated moderately to the point of softening and then cooled to ambient temperature. In this case, a net change in velocity of -1.45% was observed. In the next stage, the same portion of the sample was further heated until it began to bubble. As shown in Fig. 6(b), after again cooling the sample to ambient temperature a net change in velocity of $+1.00\%$ was observed relative to the original undamaged sample. Apparently, extreme heating caused hardening or embrittlement that raised the average velocity in the heated region of the sample. Ambient temperature effects were minor in these tests because the sample temperature was nearly the same when all test signals were acquired.

These experiments confirmed the improved method's ability to measure small permanent velocity changes due to physical alterations within the sample. Since the observed changes exceeded those we would expect for reversible temperature variations, and since we have demonstrated that we can measure both decreases and increases in velocity due to damage, we believe these tests indicate that the doublet method is versatile as well as sensitive. There are no restrictions on the nature of the physical changes occurring in the material under test, as long as it produces a change in velocity of at least $\pm 0.01\%$. It is important to note, however, that the method may not be well suited for measuring velocity changes large enough to cause the two signals to become dissimilar. It is easy to avoid this problem, though, because the coherence spectrum will indicate when the signal delay for a given time window is too large to be measured by the cross-spectral technique. Also, it may be possible to shift signals closer together before windowing and Fourier transforming so that coherence can be recovered and measurement sensitivity maintained. Visual inspection of the two signals being studied should indicate whether or not doublet analysis can be used.

V. THE AMPLITUDE-DECAY METHOD

Extending the doublet algorithm to obtain changes in Q^{-1} involves calculating spectral amplitude ratios for the same data window pairs that were used to obtain cross-spectral phase. After taking the natural logarithm of the spectral ratios and scaling by $1/f$ all data may be plotted simultaneously versus elapsed time, similar to the way the phase-derived time delays were viewed. These scaled spectral ratios can be represented as a function of elapsed time by the relation:

$$\ln\left[\frac{\|S_1(t,f)\|}{\|S_2(t,f)\|}\right]\frac{1}{f}=\frac{\ln[R_0(f)]}{f}+\pi t\Delta Q^{-1}, \qquad (6)$$

where S_1 and S_2 are the Fourier transforms versus elapsed time of the numerator and denominator signals, respectively, and $R_0=\|S_1(0,f)\|/\|S_2(0,f)\|$ is the relative source term which, in the case of true doublets, should be unity. The slope of a regression line fit to data that obey this relation is proportional to ΔQ^{-1}. In general, though, Q^{-1} may be fre-

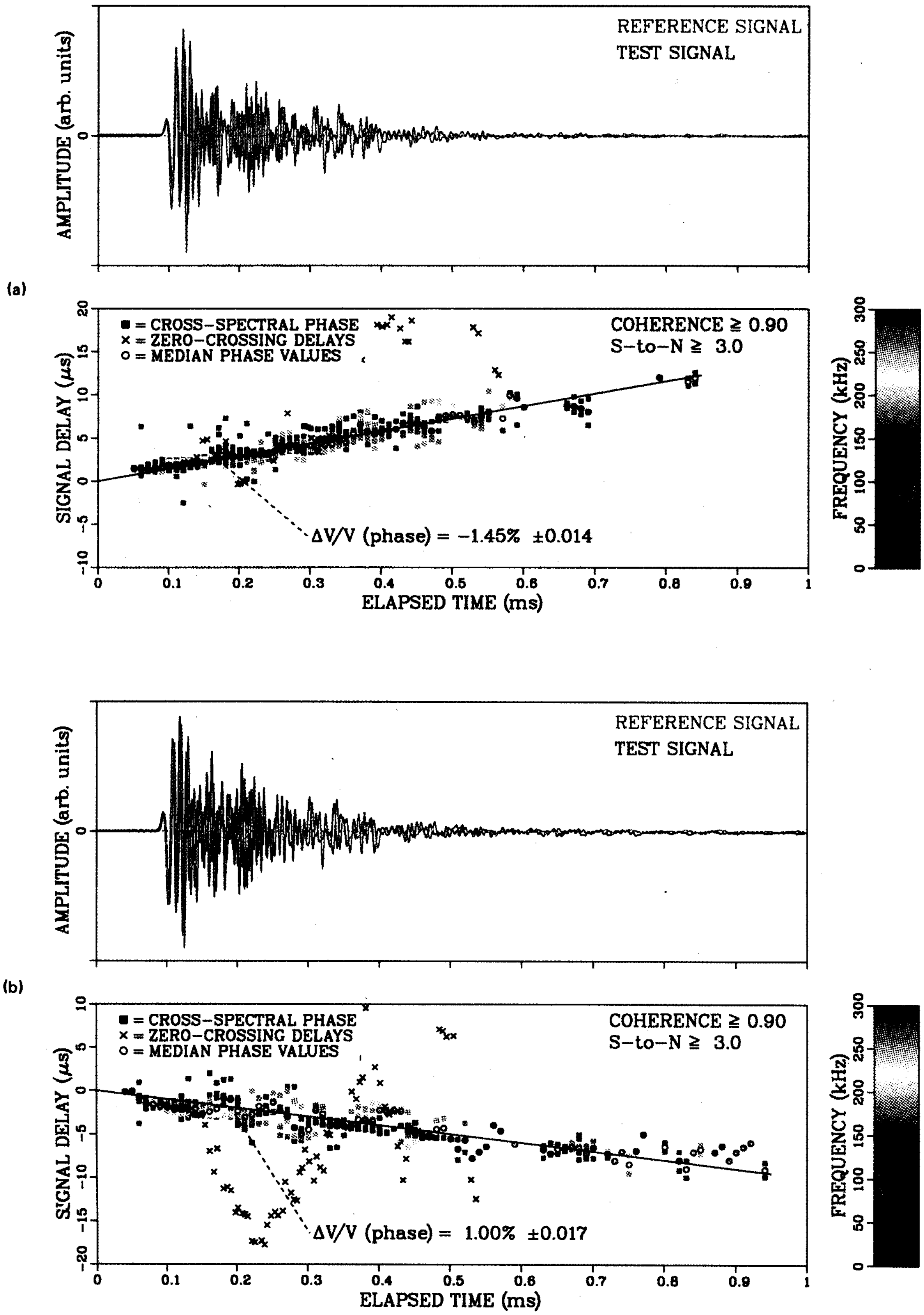

FIG. 6. (a) Results of doublet phase analysis for the first of two stages of permanent damage to the thin Plexiglas sample. Test signals were recorded before and after moderate heating of a portion of the sample to the point of softening and then cooling to ambient temperature. A net velocity decrease was observed. Zero-crossing delays were used to guide the phase unwrapping. (b) Doublet phase results for the second stage of permanent damage to the same Plexiglas sample used in (a). Test signals were recorded before and after extreme heating of the same portion of the sample to the point of bubbling and again cooling to ambient temperature. A net velocity increase was observed, relative to the original undamaged sample. Because the zero-crossing delays were so erratic, due to the complexity of the doublet signals, the median phase-derived delays were used to guide the phase unwrapping.

quency dependent over certain bands[18] and we must allow the possibility that separate fits over numerous frequencies may be necessary to fully characterize an attenuation change. We must also maintain the assumption that we are analyzing the decay of a single wave type so that we do not have to separate the effects of different waves attenuating at different rates within the same scattered wave train. Equation (6) can be applied to nondoublet data, but the results are usually difficult to interpret because of differences in source and receiver effects and uncertainties in defining the volumes sampled by the scattered waves. These uncertainties are mostly eliminated when the signals under comparison are generated by doublet events.

In Fig. 7(a), we show the amplitude-decay results for the same signals shown in Fig. 6(a), which were acquired before and after heating a portion of the thin plate to the point of softening and then cooling. The scaled spectral amplitude ratios are color coded according to frequency and we have used the same frequency and signal-to-noise cutoffs as in Fig. 6(a). In this example, the attenuation change is clearly frequency dependent because the slopes vary strongly over the frequency range of approximately 50–200 kHz. However, over the dominant frequency band of the two signals, from 75 to 150 kHz, the slopes are fairly constant and we assume here that ΔQ^{-1} should also be nearly constant over the dominant band. A discussion of possible reasons for frequency-dependent Q^{-1} changes in Plexiglas is beyond the scope of this paper. The resulting value for ΔQ^{-1} obtained by fitting the scaled ratios to Eq. (6) for the dominant band indicates that attenuation has increased due to the first stage of damage. This is consistent with the decrease in velocity observed in Fig. 6(a).

In Fig. 7(b), we show amplitude-decay results for the doublet pair shown before in Fig. 6(b) for the second stage of damage. In this case, the scaled spectral ratios do not exhibit significant frequency dependence. By fitting data to Eq. (6) for the dominant frequency band as before, we observed a net decrease in attenuation. This is consistent with the net increase in velocity observed in Fig. 6(b). Note, however, that the positive slope of the spectral ratios which led to the measured decrease in Q^{-1} does not occur until later in the coda wavetrain. This indicates that the scattered waves did not detect the region of decreased attenuation as early as the corresponding region of velocity change was detected. This phenomenon implies that identification of specific regions of change should be possible if adequate modeling of the scattered wave field can be accomplished. Note also that the regression line in Fig. 7(b) does not extrapolate back to a value of zero at the zero-time intercept, as should be the case for true doublets when a pervasive change in Q^{-1} has occurred [cf. Fig. 7(a)]. This could mean that in cases where only a portion of the sampled region has changed, the true zero intercept should be shifted out to the elapsed time at which the change in amplitude-decay rate is first detected, which is at approximately 0.35 ms in Fig. 7(b). Although the zero intercept in Fig. 7(b) may have large uncertainty, the slope of the regression line and the corresponding estimate for ΔQ^{-1} are reliable.

As opposed to the phase-delay method, which yields relative velocity changes directly, the amplitude-decay method yields absolute values for ΔQ^{-1}. To convert these measurements to a percentage change, we need an initial estimate of the background value for Q^{-1} before damaging the sample. For the undamaged Plexiglas plate, we estimated this background value by measuring the decrease in first arrival amplitude of a single source pulse recorded at progressively further receivers and correcting for geometric spreading. The value we estimated was approximately $Q^{-1} = 0.05$ (or $Q = 20$). Thus, for the example after the first stage of damage shown in Fig. 7(a), the measured change of $\Delta Q^{-1} = 0.004 \pm 0.0003$ represents a relative change in Q^{-1} of approximately 10% with a standard error of $\pm 1.0\%$. Note, however, that the measured value of ΔQ^{-1} would represent a larger percentage change for a material with an initial Q^{-1} lower than 0.05. Thus the sensitivity of the measurement may depend on the material being tested.

Other methods of measuring attenuation changes from coda waves[19] usually require repeated estimation of absolute Q^{-1} values to obtain ΔQ^{-1} versus time. Fehler *et al.*[20] used this coda-decay method to estimate temporal changes in Q^{-1} at Mount St. Helens. Typical standard errors for these absolute measurements of coda Q^{-1} are on the order of $\pm$ 20–30%. Thus any temporal changes in Q^{-1} measured by the coda-decay method would be significant only if they were on the order of 40% to 50% or larger. The use of doublets, then, represents the potential for realizing a five-fold increase in measurement sensitivity for changes in Q^{-1} and a 20-fold decrease in standard errors.

VI. DISCUSSION

As a high-sensitivity monitoring tool, the active doublet method will greatly reduce the threshold for detecting changes in velocity and Q^{-1} accompanying a large variety of important natural and man-made phenomena in the earth's crust. With further research, its potential use as a low-resolution imaging tool could also be exploited. We discuss a number of possible uses for the method in active field measurements below.

We believe the method will be particularly useful for estimating progressive changes in hydrocarbon and geothermal reservoir size which could improve predictions of production history and reservoir lifetime. This information will be valuable for estimating when secondary recovery methods will need to be initiated. Furthermore, once secondary recovery has begun, the doublet method can be used to monitor the migration of water, steam, and CO_2 flooding fronts. The fluid migration problem also has bearing on monitoring the progress of solution mining operations, assessing the integrity of waste repositories and providing guidance for cleanup operations.

A major concern in mining operations is the detection of conditions which could lead to rock failure and cave-ins. Typically the stresses involved in creating a mine failure will produce a volume expansion, or dilatancy, in the rock surrounding the mine walls which may accumulate for some time before a failure occurs. Thus it would be useful to char-

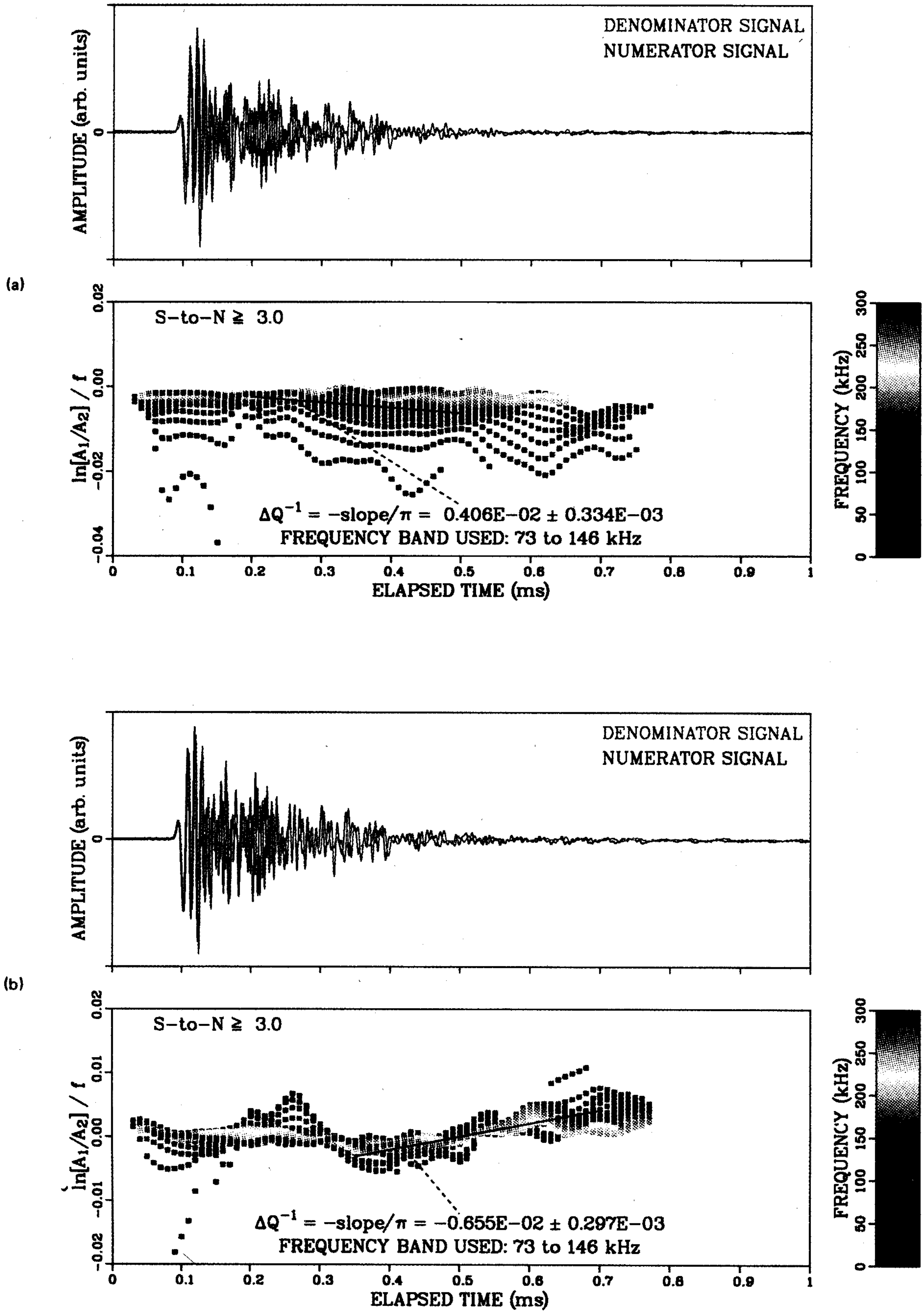

FIG. 7. (a) Results obtained with the doublet amplitude-decay method for the same signals used in Fig. 6(a). A net increase in attenuation was observed after moderate heating of the Plexiglas sample. The value for ΔQ^{-1} was obtained by fitting a regression line to the scaled ratio data over the dominant frequency band of the signals. (b) Doublet amplitude results obtained for the same signals used in Fig. 6(b). A net decrease in attenuation was observed in the later section of the coda waves after extreme heating and cooling of the Plexiglas sample.

acterize the early stages of this dilatancy so that a sensitive threshold can be set for detection of a potential failure condition. This is another possible application for the active doublet method, because permanent transducers could be cemented into mine walls so that the surrounding rock could be periodically monitored for small velocity and Q^{-1} changes which would accompany the earliest stages of dilatancy.

For volcanic hazards assessment, the active doublet method could be used to periodically monitor dormant volcanoes for early evidence of renewed magmatic activity. It could also be used to monitor active volcanoes for magma migration or inflation episodes which might indicate an impending eruption. Currently, seismic alarms for volcanoes rely on the detection and mapping of earthquake swarms associated with major changes in volcanic activity or on the onset of volcanic tremor signals which are generated by the migration of large amounts of magma. Both tremor and swarms, however, represent such major changes that it is often too late for their detection to be used as eruption alerts. With a few appropriately placed recording stations and active sources, however, the doublet method could be used to detect the earliest stages of magma migration and thus could predict where the magma is going and whether or not its destination indicates a potential hazard.

In the field of earthquake prediction, the most important information to be obtained is the precise temporal and spatial distribution of stress in and around an active fault zone. Because small stress changes cause corresponding changes in velocity and Q^{-1}, the active doublet method will be very useful for characterizing the smaller scale changes which occur at the beginning of the stress accumulation and release cycle which leads to periodic major earthquakes. Because very small variations in initial conditions at the beginning of the stress cycle may play a role in perturbing the eventual occurrence time of an earthquake, we believe the doublet method will help refine current prediction methods.

VII. CONCLUSIONS

We have developed and tested improved methods for measuring temporal changes in elastic wave velocity and attenuation in materials using active repeatable sources. The improvements allow measurements of small velocity changes to be made with significantly less user interaction and processing steps than is required by the original two-step method of Poupinet *et al.*[3] We demonstrated how easily the two-step method can produce erroneous results if the intermediate steps of the analysis are not inspected in detail to ensure that cross-spectral phase data are properly unwrapped. In contrast, the improved one-step method described here is more robust in that reliable results are typically obtained after choosing and fixing a small number of analysis parameters. We also extended the method to use relative amplitude decay rates for measuring small changes in Q^{-1}. By conducting laboratory ultrasonics experiments in Plexiglas samples, we demonstrated how the improved phase-delay algorithm succeeded in measuring velocity changes as small as 0.01% due to ambient temperature variations. We also demonstrated how the amplitude-decay method can measure ΔQ^{-1} as small as approximately 10%. Both of these measurement capabilities can be extremely valuable for monitoring the earth's crust for small precursory changes that may precede phenomena such as major earthquakes, volcanic activity, fluid migration, and rock failure.

ACKNOWLEDGMENTS

This work was supported by the Earth and Environmental Sciences Division of the Los Alamos National Laboratory, under the auspices of the United States Department of Energy. Jim Albright's encouragement and suggestions, as well as his support in procuring laboratory equipment, were crucial for allowing this work to progress. Paul Johnson's persistence in emphasizing the value of the active doublet method, as well as his experience with laboratory ultrasonics work, have provided the motivation and practical known-how for carrying out the necessary experiments for testing and improving the methods presented here. Steve Taylor reviewed the manuscript and made many useful suggestions for revisions which helped clarify the presentation of our work. We also thank the two anonymous reviewers who suggested several further improvements to the manuscript.

[1]H. Sato "A Precursorlike Change in Coda Excitation Before the Western Nagano Earthquake ($M_S = 6.8$) of 1984 in Central Japan," J. Geophys. Res. **92**, 1356–1360 (1987).

[2]Z. Wang, W. K. Hirsche, and G. Sedgwick, "Seismic Monitoring of Water Floods?—A Petrophysical Study," Geophysics **56**, 1614–1623 (1991).

[3]G. Poupinet, W. L. Ellsworth, and J. Frechet, "Monitoring Velocity Variations in the Crust Using Earthquake Doublets: An Application to the Calaveras Fault, California," J. Geophys. Res. **89**, 5719–5731 (1984).

[4]K. Aki, "Analysis of the Seismic Coda of Local Earthquakes as Scattered Waves," J. Geophys. Res. **74**, 615–631 (1969).

[5]R. W. Clymer and T. V. McEvilly, "Travel-time Monitoring with Vibroseis," Bull. Seismol. Soc. Am. **71**, 1903–1927 (1981).

[6]P. C. Leary and P. E. Malin, "Millisecond Accurate Monitoring of Seismic Travel Times over 13- and 18-Kilometer Baselines," J. Geophys. Res. **87**, 6919–6930 (1982).

[7]I. A. Viktorov, *Rayleigh and Lamb Waves: Physical Theory and Applications* (Plenum, New York, 1967), Chap. 2, pp. 67–75 [translated from Russian].

[8]H. Hamaguchi and A. Hasegawa, "Recurrent Occurrence of Earthquakes with Similar Waveforms and its Related Problems," J. Seismol. Soc. Jpn. **28**, 153–169 (1975) [in Japanese].

[9]R. J. Geller and C. S. Mueller, "Four Similar Earthquakes in Central California," Geophys. Res. Lett. **7**, 821–824 (1980).

[10]M.-J. Frémont and S. D. Malone, "High Precision Relative Locations of Earthquakes at Mount St. Helens, Washington," J. Geophys. Res. **92**, 10223–10236 (1987).

[11]W. Foxall, A. Michelini, and T. V. McEvilly, "The Parkfield Monitoring Program: Fault Zone Characteristics Revealed by High-Precision Microearthquake Locations," Seismol. Res. Lett. **60**, 32 (1989).

[12]E. Karageorgi, R. Clymer, and T. V. McEvilly, "Seismological Studies at Parkfield: II. Search for Temporal Variations in Wave Propagation using Vibroseis," submitted to J. Geophys. Res. (1991).

[13]P. M. Roberts, "Development of the Active Doublet Method for Monitoring Small Changes in Crustal Properties," Seismol. Res. Lett. **62**, 36 (1991).

[14]M. B. Priestley, *Spectral Analysis and Time Series* (Academic, San Diego, 1981), 6th printing, Chap. 9, p. 704.

[15]J. M. Tribolet, "A New Phase Unwrapping Algorithm," IEEE Trans. Acoust. Speech Signal Process. **ASSP-25**, 170–177 (1977).

[16]*CRC Handbook of Chemistry and Physics*, edited by R. C. Weast and M. J. Astle (CRC, Boca Raton, FL, 1980), 61st ed., p. C-739.

[17]A. Migliori, personal communication (1991). From Migliori's experience in measuring physical property variations with temperature, a general rule is that changes in modulus are at least an order of magnitude larger than the corresponding thermal expansion coefficient.
[18]K. Aki, "Scattering and Attenuation of Shear Waves in the Lithosphere," J. Geophys. Res. **85**, 6496–6504 (1980).
[19]W. S. Phillips and K. Aki, "Site Amplification of Coda Waves from Local Earthquakes in Central California," Bull. Seismol. Soc. Am. **76**, 627–648 (1986).
[20]M. Fehler, P. M. Roberts, and T. Fairbanks, "A Temporal Change in Coda Wave Attenuation Observed During an Eruption of Mount St. Helens," J. Geophys. Res. **93**, 4367–4373 (1988).